

NONLOCAL ADHESION MODELS FOR MICROORGANISMS ON BOUNDED DOMAINS *

THOMAS HILLEN[†] AND ANDREAS BUTTENSCHÖN[‡]

Abstract. In 2006 Armstrong, Painter and Sherratt formulated a non-local differential equation model for cell-cell adhesion. For the one dimensional case we derive various types of adhesive, repulsive, and no-flux boundary conditions. We prove local and global existence and uniqueness for the resulting integro-differential equations. In numerical simulations we consider adhesive, repulsive and neutral boundary conditions and we show that the solutions mimic known behavior of fluid adhesion to boundaries. In addition, we observe interior pattern formation due to cell-cell adhesion.

Key words. cell-cell adhesion, non-local models, no-flux boundary conditions, global existence, semigroups

AMS subject classifications. 92C17, 35Q92, 35K99

1. Introduction. Adhesion between cells and other tissue components are fundamental in tissue development (embryogenesis), and homeostasis and repair of tissues. Cellular adhesion allow cells to self-organize by exerting forces on each other. A single adhesive cell population, for instance, will aggregate to form sheets or aggregates, while two cell populations “sort” into one of four cell-sorting configurations, first described by Steinberg [27]. The regulation of cellular adhesion is critical in both development and pathological conditions such as cancer. For many cancers the loss of cell-cell cohesion is a pre-requisite for cell invasion and subsequent metastasis formation. Due to their biological importance, it is highly desirable to have accurate models of cellular adhesion as part of standard modelling frameworks. Here we consider models of the reaction-diffusion-taxis form, which are popular in the modelling of biological tissues.

In 2006, Armstrong *et al.* [4] proposed the first successful continuum model of cellular adhesion. The novelty of this model is the use of a non-local integral term to describe the adhesive forces between cells. To introduce the model, we let $u(x, t)$ denote a cell density at spatial location x and time t , then on the real line the model is given by the following non-local partial differential equations.

$$(1.1) \quad u_t(x, t) = Du_{xx}(x, t) - \alpha \left(u(x, t) \int_{-R}^R H(u(x+r, t)) \Omega(r) dr \right)_x,$$

where D is the diffusion coefficient, α the strength of homotypic cell adhesion, $H(u)$ is a possibly nonlinear function describing the nature of the adhesion force, $\Omega(r)$ is an odd function giving the adhesion force’s direction and R the sensing radius of the cell. The model (1.1) was derived from an underlying stochastic random walk in [8].

The novelty of model (1.1) is the integral term modelling cell-cell adhesion. Intuitively, the integral term can be interpreted as a tug-of-war, or a force balance causing cells to move in the direction of largest adhesion force. Since other cells are required for the creation of adhesive forces, it is easy to see that the non-local term causes cells

*Submitted to the editors DATE.

[†]Department of Mathematical and Statistical Sciences, Centre for Mathematical Biology, University of Alberta, Edmonton T6G 2G1, AB, Canada (thillen@ualberta.ca, <http://ualberta.ca/~thillen/>).

[‡]Department of Mathematics, University of British Columbia, Vancouver V6T 1Z2, BC, Canada (abuttens@math.ubc.ca, www.buttenschoen.ca).

to aggregate. Furthermore the two cell population version of model (1.1) is the first continuum model to replicated the different cell-sorting experiments from Steinberg's classical experiments [4].

In biological systems, cellular adhesion features prominently in organism development, wound-healing, and cancer invasion (metastasis). Therefore, it is unsurprising that model (1.1) has been extensively used to model cancer cell invasion [15, 26, 16, 23, 10, 2, 11, 6], and developmental processes [5, 24]. To allow for numerical exploration, Gerisch et al. [14] developed an efficient numerical method for the integral term in (1.1). Finally, with the availability of controlled biological experiments [19, 9] extended the adhesion model (2.1) with density-dependent diffusion, and volume filling to improve the model's fit to experimental data.

Existence results for the solutions of the non-local equation (1.1) were developed in [26, 2, 18]. Most significant is the general work by Hillen *et al.* [18], who showed local and global existence of classical solutions in unbounded domains. Finally, for small values of adhesion strength α , travelling wave solutions of the non-local adhesion model have been described in [21].

All of the above mentioned models and results considered models on unbounded or periodic domains, since this avoids defining the non-local adhesion operator near boundaries. In this paper, we extend model (1.1) to a bounded domain. Our work is motivated by observations that adhesive or repulsive cell-boundary interactions are significant during development. For instance, repulsive membranes are required for correct organ placement in zebrafish [25]. In this work, we formulate different biological boundary conditions for model (1.1), describing adhesive, repulsive, or neutral boundary interactions. Due to the non-locality we find that it is not sufficient to describe the non-local operators behaviour on just the boundary, but its behaviour must be provided in a boundary region.

Another class of non-local models for species aggregations are the so called *aggregation equations* [12, 29]. Here the non-local term arises through an interaction potential between different individuals. This interaction potential can describe long range attraction, short range repulsion and intermediate range alignment of species. There is an extensive mathematical theory related to the aggregation equations, and most of the results rely on the fact that the aggregation equations arise as gradient flow of a potential. Our adhesion model (1.1) does not have such a variational structure. The aggregation equations on a bounded domain have recently been studied in [12, 29]. The boundary conditions are very similar to our adhesive and repulsive boundary conditions.

1.1. Outline. Starting from model (1.1) in divergence form, in section 2 we formulate several biologically relevant boundary conditions. In particular, we consider two cases (1) the adhesive flux is independent from the diffusive flux and (2) the diffusive and adhesive flux depend on each other. In the case, of independent fluxes, using semi-group theory, we develop a local existence theory (section 3) and global existence (section 4) for the non-local adhesion model with no-flux boundary conditions. In section 5 we compare numerical solutions of the adhesion model with different no-flux boundary conditions to the periodic situation. We observe boundary adhesion effects, similar to those known from thin film wetting of glass boundaries. The case where the adhesive and diffusive fluxes are coupled leads to non-trivial Robin-type boundary conditions. An existence theory for those cases is much more involved and left for future research. In section 6 we provide some concluding remarks, and outlooks for future work.

2. Boundary conditions for non-local operators. We consider the one-dimensional Armstrong adhesion model on the interval $[0, L]$ with sensing radius $0 < R < \frac{L}{2}$.

$$(2.1) \quad u_t(x, t) = Du_{xx}(x, t) - \alpha \left(u(x, t) \int_{E(x)} H(u(x+r, t)) \Omega(r) dr \right)_x,$$

and we define the non-local integral operator as

$$(2.2) \quad \mathcal{K}[u](x, t) = \int_{E(x)} H(u(x+r, t)) \Omega(r) dr.$$

The domain of integration $E(x) \subset [-R, R]$ is chosen to ensure that the integrand does not reach outside of the domain $[0, L]$, and it is called the *sampling domain*. The sampling domain is not unique and we give several examples in [subsection 2.1](#).

To address the boundary conditions we consider the particle flux

$$(2.3) \quad J(x, t) = Du_x(x, t) - \alpha u(x, t) \mathcal{K}[u](x, t).$$

Our first goal is to formulate no-flux boundary conditions i.e. $J(x, t) = 0$ for $x = 0, L$. We consider two different cases; (1) the diffusive flux and the adhesive flux are independent on the boundary (2) the diffusive and adhesive flux depend on each other.

Independent case. If we stipulate that the diffusive and adhesive component of the flux are independently zero on the boundary, then the following are a suitable set of boundary conditions for [\(2.1\)](#).

$$(2.4) \quad u_x(0, t) = u_x(L, t) = 0,$$

$$(2.5) \quad \mathcal{K}[u](0) = \mathcal{K}[u](L) = 0.$$

The first condition [\(2.4\)](#) is a condition on the solution $u(x, t)$ and we can include this into the right choice of function space. The second condition [\(2.5\)](#), however, should be seen as a condition on the non-local operator \mathcal{K} i.e. condition [\(2.5\)](#) must hold for any u . In other words, in this no-flux situation we only consider non-local operators \mathcal{K} that satisfy [\(2.5\)](#). We give explicit examples later.

Dependent case. If we want to describe adhesion to or repulsion from the boundaries, we can relax the above conditions on \mathcal{K} . For example if we assume

$$(2.6) \quad \mathcal{K}[u](0) < 0, \quad \mathcal{K}[u](L) > 0,$$

then we have net flow towards the boundaries, i.e. an adhesive boundary, while

$$(2.7) \quad \mathcal{K}[u](0) > 0, \quad \mathcal{K}[u](L) < 0,$$

denote repulsive boundary conditions. However, to ensure that the total particle flux $J(x, t)$ is zero on the boundary we require that the diffusive flux component counteract the adhesive component, that is

$$(2.8) \quad Du_x(x, t) = \alpha u(x, t) \mathcal{K}[u](x, t), \quad \text{for } x = 0, L.$$

This results in a non-local boundary condition of Robin type.

Case	$\mathcal{K}[u]$	$f_1(x)$	$f_2(x)$
periodic	$\int_{E(x)} H(u)\Omega(r) \, dr$	$f_1 = -R$	$f_2 = R$
naive	$\int_{E(x)} H(u)\Omega(r) \, dr$	$f_1 = \begin{cases} -x, & I_1 \\ -R, & I_2 \end{cases}$	$f_2 = \begin{cases} R, & I_3 \\ L - x, & I_4 \end{cases}$
non-flux	$\int_{E(x)} H(u)\Omega(r) \, dr$	$f_1 = \begin{cases} R - 2x, & I_1 \\ -R, & I_2 \end{cases}$	$f_2 = \begin{cases} R, & I_3 \\ 2L - R - 2x, & I_4 \end{cases}$
weakly adhesive	$\int_{E(x)} H(u)\Omega(r) \, dr + a_0 + a_L$ $a_0 = \beta^0 \int_{-R}^{-x} \Omega(r) \, dr$ $a_L = \beta^L \int_{L-x}^R \Omega(r) \, dr$	$f_1 = \text{naive}$	$f_2 = \text{naive}$

Table 1: The different cases of suitable boundary conditions on $[0, L]$. The sensing slice is defined as $E(x) = \{r \in [-R, R] : f_1(x) \leq r \leq f_2(x)\}$. The abbreviations I_1, I_2, I_3, I_4 stand for $x \in [0, R], x \in (R, L], x \in [0, L - R], x \in (L - R, L]$, respectively.

2.1. Examples. We consider several examples of sensing domains $E(x)$ for use in the non-local operator $\mathcal{K}[u]$ defined in equation (2.2). The examples are summarized in Table 1.

Example 2.1 (periodic). The periodic case is special, since $x = 0$ and $x = L$ are identified. Any integral over a domain of length $2R$ is well defined. This case is included in our framework with the choice of sampling domain of

$$E_1(x) = [-R, R].$$

and periodic boundary conditions.

Example 2.2 (naive). The first idea of a well defined integral operator (2.2) on $[0, L]$ is to remove those parts of the integration that leave the domain. This can be achieved through the sampling slice

$$E_2(x) = \{r \in [-R, R], f_1(x) \leq r \leq f_2(x)\}$$

with

$$f_1(x) = \begin{cases} -x, & x \in [0, R] \\ -R, & x \in (R, L] \end{cases}, \quad f_2(x) = \begin{cases} R, & x \in [0, L - R] \\ L - x, & x \in [L - R, L] \end{cases}.$$

At the left boundary we obtain

$$\mathcal{K}[u](0) = \int_0^R H(u(x+r, t))\Omega(r) \, dr \geq 0,$$

which is non-negative for positive H and Ω . Similarly we find $\mathcal{K}[u](L) \leq 0$. In this situation cells at the boundary are attracted by cells in the interior with no interaction with the wall. Hence a net flow away from the boundary is created. By equation (2.7), we classify these naive boundary conditions as repulsive. Further, this implies that $E_2(x)$ are not suitable to ensure that $\mathcal{K}[u]$ are zero on the boundary for all u . For a pictorial representation of the sampling domain $E_2(x)$ see Figure 2.

Example 2.3 (no-flux). In this example we choose the sampling domain such that the sampling domain $E(x)$ is a set of measure zero for $x = 0, L$, thus ensuring that $\mathcal{K}[u]$ is zero on the boundary. We let

$$E_3(x) = \{r \in [-R, R], f_1(x) \leq r \leq f_2(x)\},$$

where now

$$f_1(x) = \begin{cases} R - 2x, & x \in [0, R] \\ -R, & x \in (R, L] \end{cases}, \quad f_2(x) = \begin{cases} R, & x \in [0, L - R] \\ 2L - R - 2x, & x \in [L - R, L] \end{cases}.$$

In this case we obtain on the left boundary

$$\mathcal{K}[u](0) = \int_R^R H(u(x+r, t)) \Omega(r) dr = 0,$$

and $\mathcal{K}[u](L) = 0$, and hence condition (2.5) is satisfied. This makes $E_3(x)$ a suitable sampling domain for the independent no-flux boundary conditions. In this situation cell protrusions which hit the boundary fold back onto the cell itself, thus neutralizing the cell's adhesion molecules (see Figure 1 (A)).

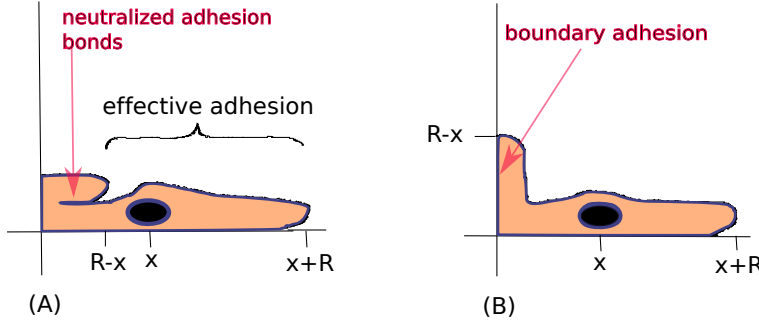


Fig. 1: (A): The filopodia of cell are reflected or stopped at the boundary. As a result the cell starts to form adhesion bonds with itself, which are then not contributing to the net adhesion force. Note that only one cell is shown in this sketch. (B) The weak adhesive case. Cells make contact to the boundary in a well balanced way, such that the net flux is still zero.

Inspired by the previous examples we define a whole class of suitable sampling domain $E(x)$ as follows.

DEFINITION 2.4 (Sampling domain).

1. Two continuous functions $f_{1,2} : D \rightarrow \mathbb{R}$ define a suitable sampling domain $E(x)$ if they satisfy
 - (a) $-R \leq f_1(x) \leq f_2(x) \leq R$ for all $x \in [0, L]$.
 - (b) $f_1(x) = -R$ for $x \in [R, L]$
 - (c) $f_2(x) = R$ for $x \in [0, L - R]$.
 - (d) $f_1(x)$ and $f_2(x)$ are non-increasing and have uniformly bounded one-sided derivatives.
2. A suitable sampling domain $E(x)$ satisfies condition (2.5) if in addition

$$(e) \quad f_1(0) = R \quad \text{and} \quad f_2(L) = -R.$$

It is straight forward to check that all our sampling domain are suitable. However, only $E_3(x)$ satisfies condition (2.5). In Figures 2 and 3 we show two examples of sampling domains over the whole domain $[0, L]$.

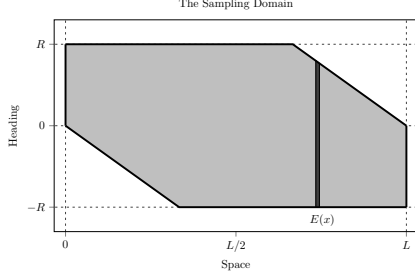


Fig. 2: A plot of the naive sensing domain $E_2(x)$ see Example 2.2.

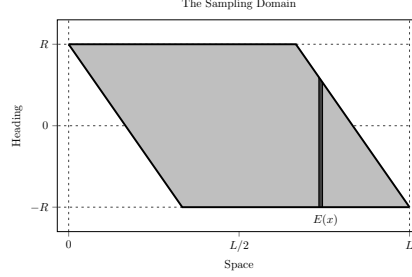


Fig. 3: A plot of the no flux sensing domain $E_3(x)$ see Example 2.3.

Example 2.5 (Adhesive / Repulsive). The framework developed here can be used to explicitly model adhesion or repulsion by the domain boundary. For that we assume that the interaction force with the boundary is proportional to the extent of cell protrusions that attach to the boundary, which corresponds to the amount of cell protrusion that would reach out of the domain if there was no boundary (see Figure 1 (B)). For example at $x \in (0, R)$. If the cell extends to $x - R$, then the interval $[x - R, 0]$ is outside of the domain. We assume that instead of leaving the domain, the protrusion interacts with the boundary, given boundary adhesion terms of the form

$$\begin{aligned} a^0(x) &:= \beta^0 \int_{-R}^{-x} \Omega(r) \, dr, & x \in [0, R) \\ a^L(x) &:= \beta^L \int_{L-x}^L \Omega(r) \, dr, & x \in (L - R, L] \end{aligned}$$

where β^0 and β^L are constants of proportionality. $\beta^0, \beta^L > 0$ describes boundary adhesion, while $\beta^0, \beta^L < 0$ describes boundary repulsion.

In this case we define the adhesion operator as linear combination of all relevant adhesive effects. Using indicator functions $\chi_A(r)$ we can write

$$\begin{aligned} \mathcal{K}[u](x, t) &= \int_{E(x)} H(u(x + r, t)) \Omega(r) \, dr \\ &\quad + \beta^0 \chi_{[0, R]}(x) \int_{-R}^{-x} \Omega(r) \, dr + \beta^L \chi_{[L-R, L]}(x) \int_{L-x}^L \Omega(r) \, dr \\ (2.9) \quad &= \int_{-R}^R (\chi_{E(x)} H(u(x + r, t)) + \beta^0 \chi_{[-R, -x]}(x) + \beta^L \chi_{[L-x, R]}) \Omega(r) \, dr, \end{aligned}$$

where we omitted the r -dependence in the indicator functions for brevity. Here $E(x)$ is any suitable sampling domain as defined in Definition 2.4. Further we note that whenever

$$\beta^0 = \frac{1}{2} \int_{E(0)} H(u(r, t)) \Omega(r) \, dr,$$

a similar expression can be found for β^L , then $\mathcal{K}[u]$ satisfies condition (2.5).

Example Summary. To combine all different possible examples, we define a general integral operator as

$$(2.10) \quad \mathcal{K}[u](x, t) = \int_{-R}^R F(u(x+r, t), x, r) \Omega(r) \, dr,$$

with

$$(2.11) \quad \begin{array}{ll} \text{periodic} & F(u, x, r) = H(u(x+r, t)) \\ \text{naive case} & F(u, x, r) = \chi_{E_2(x)} H(u(x+r, t)) \\ \text{non-flux} & F(u, x, r) = \chi_{E_3(x)} H(u(x+r, t)) \\ \text{general case} & F(u, x, r) = \chi_{E(x)} H(u(x+r, t)), \quad E(x) \text{ is suitable} \\ \text{bdy interac.} & F(u, x, r) = \chi_{E(x)} H(u(x+r, t)) + \beta^0 \chi_{[-R, -x]} + \beta^L \chi_{[L-x, R]} \\ & E(x) \text{ is suitable, } \beta^0, \beta^L \text{ are constants,} \end{array}$$

where “bdy interac.” stands for “adhesive or repulsive interaction with the boundary”. We will summarize general assumptions on F in the next section.

3. Local Existence and Uniqueness. We consider non-local adhesion models on a one-dimensional bounded domain $[0, L]$ with independent no-flux boundary condition:

$$(3.1) \quad \left\{ \begin{array}{ll} u_t(x, t) & = \quad Du_{xx}(x, t) - \alpha (u(x, t) \mathcal{K}[u](x, t))_x \\ \mathcal{K}[u](x, t) & = \quad \int_{-R}^R F(u(x+r, t), x, r) \Omega(r) \, dr \\ u(x, 0) & = \quad u_0(x) \geq 0 \\ 0 & = \quad u_x(0, t) = u_x(L, t) \\ \mathcal{K}[u](x) & \text{satisfies condition (2.5).} \end{array} \right.$$

We introduce the function space

$$\mathcal{Y} := \left\{ u \in H^1[0, L] : \int_0^L u(x) \, dx = m_0 \right\},$$

where $m_0 = \int_0^L u_0(x) \, dx$. We recall that the function space \mathcal{Y} can be identified with the quotient space H^1/\mathbb{R} . We then pick the solution of equation (3.1) to be the representative with mass m_0 . From [20] we recall that this quotient space is Hilbert, and that its norm $|u|_{H^1/\mathbb{R}}$ is equivalent to the norm

$$||u|| := \left(\int_0^L u_x^2 \, dx \right)^{1/2}.$$

We make the following general assumptions:

- (A1) $u_0 \in \mathcal{Y}$, $\mathcal{X} = \mathcal{C}^0([0, T], \mathcal{Y} \cap L^\infty(0, L))$, $T > 0$.
- (A2) $\Omega(r) = \frac{r}{|r|} \omega(r)$, $\omega(r) = \omega(-r)$, $\omega(r) \geq 0$, $\omega(R) = 0$, $R > 0$.
- (A3) $V = [-R, R]$, $\omega \in L^1(V) \cap L^\infty(V)$, $\|\omega\|_{L^1[0, R]} = \frac{1}{2}$.

(A4) For each $x \in [0, L]$, $r \in [-R, R]$ the kernel $F(u, x, r)$ is linearly bounded in u and differentiable in u with uniformly bounded and Lipschitz continuous derivative:

$$|F(u, x, r)| \leq k_1(1 + |u|), \quad \left| \frac{\partial}{\partial u} F(u, x, r) \right| \leq k_2.$$

$$\left| \frac{\partial}{\partial u} F(u, x, r) - \frac{\partial}{\partial u} F(v, x, r) \right| \leq k_3|u - v|.$$

(A5) $F(u, x, r)$ is piecewise continuous as a function of r .

(A6) $x \mapsto \int_V F \Omega(r) dr$ is differentiable in x with a bounded derivative. There are two constants $k_4, k_5 > 0$ such that

$$\begin{aligned} \left| \frac{\partial}{\partial x} \int_V F(u(x+r, t), x, r) \Omega(r) dr \right|_2 &\leq k_4(1 + |u(\cdot, t)|_\infty) \\ &\leq k_5(1 + |u(\cdot, t)|_{H^1}), \end{aligned}$$

for all $u \in \mathcal{X}, t > 0$.

LEMMA 3.1. Assume (A1)–(A3). Further assume that

(A4') $H(u)$ is linearly bounded with uniform bounded and Lipschitz continuous derivative.

Then all of the above examples (2.11) satisfy assumptions (A1)–(A6).

Proof. The u -dependence in the examples (2.11) enters only through $H(u)$. Hence assumption (A4') immediately implies assumption (A4). Since u is continuous and H is continuous and the indicator functions are piecewise continuous, then also $r \mapsto F(u, x, r)$ is piecewise continuous, i.e. (A5). The critical condition to show is assumption (A6). For this we consider the case of adhesive and repulsive boundary conditions, as this proof also includes the proof of (A6) for the other examples. We have

$$F(u, x, r) = \chi_{E(x)} H(u(x+r, t)) + \beta^0 \chi_{[-R, -x]} + \beta^L \chi_{[L-x, R]}.$$

Since $E(x) = \{r \in [-R, R] : f_1(x) \leq r \leq f_2(x)\}$ is a suitable slice, we can compute the distributional derivative of F . We divide this into several steps. Differentiating the integral term, we find

$$(3.2) \quad \frac{\partial}{\partial x} \int_V F(x, u, r) \Omega(r) dr = \int_V [F_u(u, x, r) u_x + F_x(u, x, r)] \Omega(r) dr.$$

We use assumption (A4) to estimate the first term

$$\left| \int_V F_u(u, x, r) u_x(x+r, t) \Omega(r) dr \right|_2 \leq k_2 |\Omega|_\infty |u_x|_2.$$

The second term is more delicate. First we compute the distributional derivative $F_x(u, x, r)$ for $r \in [-R, R]$ and $x \in [0, L]$:

$$\begin{aligned} F_x(u, x, r) &= H(u) [\mathcal{H}(r - f_1(x)) \delta(f_2 - r) f_2'(x) - \mathcal{H}(f_2 - r) \delta(r - f_1) f_1'(x)] + \\ &\quad \chi_{E(x)}(r) \frac{\partial H}{\partial x} + \beta^L \delta(r - L + x) - \beta^0 \delta(-x - r), \end{aligned}$$

where \mathcal{H} is the heaviside function. We note that $H_x = 0$ (since we are only taking the partial with respect to x now). Integrating this term with weight $\Omega(r)$ over $V = [-R, R]$, and noting that $x \in [0, L]$, we get

$$\begin{aligned} & \int_V F_x(u, x, r) \Omega(r) \, dr \\ &= H(u(x + f_2(x)) f_2'(x) \Omega(f_2(x)) - H(u(x + f_1(x))) f_1'(x) \Omega(f_1(x)) \\ & \quad - \beta^0 \chi_{[0, R)}(x) \Omega(-x) + \beta^L \chi_{(L-x, L]}(x) \Omega(L-x). \end{aligned}$$

Notice that all terms in the above expression only arise for x close to the boundaries. The terms involving $\beta^{0, L}$ are multiplied by the indicator functions of the boundary region, while the other two terms are zero outside the boundary region, since $f'_{1,2}(x) = 0$ (see Definition 2.4). Using this term we can estimate the second term in equation (3.2) by

$$\left| \int_V F_x(u, x, r) \Omega(r) \, dr \right|_2 \leq \left(2k_1 D(1 + |u|_\infty) + |\beta^0| + |\beta^L| \right) |\Omega|_\infty,$$

where $D := \max(|f'_1|_\infty, |f'_2|_\infty)$. Together we find two constants $k_4, k_5 > 0$ such that

$$(3.3) \quad \left| \frac{d}{dx} \int_V F(u(x+r, t), x, r) \Omega(r) \, dr \right|_2 \leq k_4 (1 + |u|_\infty)$$

$$(3.4) \quad \leq k_5 (1 + |u|_{H^1}),$$

□

where the last estimate follows from the Sobolev embedding.

We denote the solution semigroup $S(t)$ of the heat equation with homogeneous no-flux boundary conditions

$$\begin{cases} u_t &= Du_{xx} \\ 0 &= u_x(0, t) = u_x(L, t) \end{cases}.$$

And we can write the formal solution of (3.1) as a mild solution

DEFINITION 3.2. $u \in \mathcal{X}$ is called a mild solution of (3.1) if

$$(3.5) \quad u(x, t) = S(t)u_0 - \alpha \int_0^t S(t-s) \left(u \int_V F(u(x+r, s), x, r) \Omega(r) \, dr \right)_x \, ds.$$

THEOREM 3.3. Assume (A1)–(A6). For $T > 0$ small enough there exists a unique mild solution $u \in \mathcal{X}$ of (3.1).

Proof. Using this definition we can define a map $Q : \mathcal{X} \rightarrow \mathcal{X}$, where given $v \in \mathcal{X}$, $u = Qv$ denotes the function

$$(3.6) \quad u(x, t) = S(t)u_0 - \alpha \int_0^t S(t-s) \left(v \int_V F(v(x+r, s), x, r) \Omega(r) \, dr \right)_x \, ds.$$

We will show that this map has a unique fixed point in \mathcal{X} . Assume $v \in \mathcal{X}$. By the Sobolev embedding this implies that $v \in \mathcal{C}^0([0, T], \mathcal{C}^0([0, L]))$.

Step 1: For given $M > 2 \max\{|u_0|_{H^1}, |u_0|_\infty\}$ let $B_M(0) \subset H^1[0, L] \cap L^\infty(0, L)$ denote the ball of radius M in $H^1 \cap L^\infty$. Let $W = \mathcal{C}^0([0, T], B_M(0))$, then we show that for $T > 0$ small enough we have $Q : W \rightarrow W$. In the following estimates we ignore the arguments of the functions and we write $v = v(x, t)$, $F = F(v(x+r, s), x, s)$, and $\Omega = \Omega(r)$. The crucial term is the integral term in equation (3.6)

$$\left(v \int_V F \Omega \, dr \right)_x = v_x \int_V F \Omega \, dr + v \frac{d}{dx} \int_V F \Omega \, dr.$$

Then

$$\begin{aligned} \left| \left(v \int_V F \Omega \, dr \right)_x \right|_2 &\leq \left| v_x \int_V F \Omega(r) \, dr \right|_2 + \left| v \frac{d}{dx} \int_V F \Omega(r) \, dr \right|_2 \\ &\leq k_1 |v_x|_2 (1 + |v|_\infty) \int_V |\Omega(r)| \, dr + k_5 |v|_\infty (1 + |v|_{H^1}) \\ &\leq \kappa (1 + |v|_{H^1}) (1 + |v|_\infty) \\ (3.7) \quad &\leq \kappa (1 + M)^2, \end{aligned}$$

with $\kappa > 0$ and we used $\int_V |\Omega(r)| \, dr = 1$.

Now the heat solution semigroup regularizes [1]

$$(3.8) \quad S(t) : L^2[0, L] \rightarrow H^1[0, L] \text{ with norm } Ct^{-1/2}.$$

Hence

$$\begin{aligned} \left| \int_0^t S(t-s) \left(v \int_V F \Omega \, dr \right)_x \, ds \right|_{H^1} &\leq \kappa (1 + M)^2 \left| \int_0^t C(t-s)^{-1/2} \, ds \right| \\ &= 2\kappa C (1 + M)^2 \sqrt{t}. \end{aligned}$$

Then from (3.6) and the choice of M we find that

$$|u|_{H^1} \leq \frac{M}{2} + 2\kappa\alpha C (1 + M)^2 \sqrt{t},$$

and

$$\frac{M}{2} + 2\kappa\alpha C (1 + M)^2 \sqrt{t} < M$$

for all

$$t < M^2 (4\kappa\alpha C (1 + M)^2)^{-2}.$$

Step 2: Now we show that Q is a contraction on W for small enough time. Given $v_1, v_2 \in W$, let $u_1 = Qv_1$ and $u_2 = Qv_2$ and we abbreviate $F_1 = F(v_1(x+r, t), x, r)$ and $F_2 = F(v_2(x+r, t), x, r)$. We estimate for the H^1 -norm:

$$\begin{aligned}
|u_1 - u_2|_{H^1} &\leq \alpha \left| \int_0^t S(t-s) \left[\left(v_1 \int_V F_1 \Omega \, dr \right)_x - \left(v_2 \int_V F_2 \Omega \, dr \right)_x \right] \, ds \right|_{H^1} \\
&\leq \alpha \left| \int_0^t S(t-s) \left((v_1 - v_2) \int_V F_1 \Omega \, dr \right)_x \, ds \right|_{H^1} \\
&\quad + \alpha \left| \int_0^t S(t-s) \left(v_2 \int_V (F_1 - F_2) \Omega \, dr \right)_x \, ds \right|_{H^1} \\
&\leq \alpha \left| \int_0^t S(t-s) (v_1 - v_2)_x \int_V F_1 \Omega \, dr \, ds \right|_{H^1} \\
&\quad + \alpha \left| \int_0^t S(t-s) (v_1 - v_2) \frac{d}{dx} \int_V F_1 \Omega \, dr \, ds \right|_{H^1} \\
&\quad + \alpha \left| \int_0^t S(t-s) v_{2,x} \int_V (F_1 - F_2) \Omega \, dr \, ds \right|_{H^1} \\
&\quad + \alpha \left| \int_0^t S(t-s) v_2 \int_V (F_{1u} - F_{2u}) v_{1x} \Omega \, dr \, ds \right|_{H^1} \\
&\quad + \alpha \left| \int_0^t S(t-s) v_2 \int_V F_{2u} (v_{1x} - v_{2x}) \, dr \, ds \right|_{H^1} \\
&=: I_1 + I_2 + I_3 + I_4 + I_5.
\end{aligned}$$

We use the previous bounds of $|v_1|_{\mathcal{X}}, |v_2|_{\mathcal{X}} \leq M$ and (3.7) to study each term separately. We also use the regularization of the heat equation semigroup (3.8) for all terms I_k . We obtain

$$\begin{aligned}
I_1 &\leq \alpha \sqrt{t} (1 + M) |v_1 - v_2|_{\mathcal{X}} \\
I_2 &\leq \alpha \sqrt{t} (1 + M) k_5 |v_1 - v_2|_{\mathcal{X}} \\
I_3 &\leq \alpha \sqrt{t} M k_2 |v_1 - v_2|_{\mathcal{X}} \\
I_4 &\leq \alpha \sqrt{t} M^2 k_3 |v_1 - v_2|_{\mathcal{X}} \\
I_5 &\leq \alpha \sqrt{t} M k_2 |v_1 - v_2|_{\mathcal{X}}.
\end{aligned}$$

Which means that there is a constant $C > 0$ such that

$$|u_1 - u_2|_{H^1} \leq C \sqrt{t} |v_1 - v_2|_{\mathcal{X}}.$$

Note that since in one-dimension we have that $H^1 \subset L^\infty$ we automatically have the same estimate for the supremum norm. Together we find a constant $C > 0$ such that

$$|u_1 - u_2|_{\mathcal{X}} \leq C \sqrt{t} |v_1 - v_2|_{\mathcal{X}}, \quad \square$$

which is a contraction for t small enough.

Step 3: The map Q is a continuous contraction on $B_M(0)$ for small enough times, hence there exists a unique short-time mild solution of (3.5).

4. Global Existence.

LEMMA 4.1. Assume (A1)–(A6) and let $u(x, t)$ denote the unique, non-negative, mild solution of (3.1) from Theorem 3.3. Then there is a constant $c_1 > 0$ such that

$$(4.1) \quad |u(\cdot, t)|_2 \leq |u_0|_2 e^{c_1 t},$$

for as long as the solution exists.

Proof. We multiply (3.1) by u and integrate:

$$\begin{aligned}
\frac{d}{dt} \int \frac{u^2}{2} dx &= -D \int u_x^2 dx + \alpha \int u_x \left(u \int_V F(u, x, r) \Omega(r) dr \right) dx \\
&\leq -D \int u_x^2 dx + \frac{\alpha \varepsilon}{2} \int u_x^2 dx + \frac{\alpha}{2\varepsilon} \int \left(u \int_V F(u, x, r) \Omega(r) dr \right)^2 dx \\
&\leq \left(-D + \frac{\alpha \varepsilon}{2} \right) \int u_x^2 dx + \frac{\alpha}{2\varepsilon} \int \left[u \int_V k_1(1 + |u|) \Omega(r) dr \right]^2 dx \\
&\leq \left(-D + \frac{\alpha \varepsilon}{2} \right) \int u_x^2 dx + \frac{\alpha}{2\varepsilon} \int u^2 \left[k_1(2R + |u|_1) |\Omega|_\infty \right]^2 dx \\
&\leq \left(-D + \frac{\alpha \varepsilon}{2} \right) \int u_x^2 dx + \left[\frac{\alpha}{2\varepsilon} (2R + m_0) |\Omega|_\infty \right]^2 \int u^2 dx.
\end{aligned}$$

We choose $\varepsilon = 2D/\alpha$, such that the first term cancels and we obtain

$$\frac{d}{dt} \int \frac{u^2}{2} dx \leq \left[\frac{k_1 \alpha^2}{4D} (2R + m_0) |\Omega|_\infty \right]^2 \int u^2 dx.$$

Hence there is a constant $c_1 > 0$ such that (4.1) is satisfied. \square

THEOREM 4.2. Assume (A1)–(A6) and let $u(x, t)$ denote the unique, non-negative, mild solution of (3.1) from Theorem 3.3. Then the solution exists globally in time and there are constants $c_2, c_3 > 0$ such that

$$(4.2) \quad \|u(\cdot, t)\| \leq c_2(\|u_0\| + t)e^{c_3 t}.$$

Proof. We multiply (3.1) by u_{xx} and integrate:

$$\begin{aligned}
\frac{d}{dt} \int \frac{u_x^2}{2} dx &= \int u_x u_{xt} dx = - \int u_{xx} u_t dx \\
&= -D \int u_{xx}^2 dx + \alpha \int u_{xx} \left(u \int_V F(u, x, r) \Omega(r) dr \right)_x dx \\
(4.3) \quad &\leq \left(-D + \frac{\alpha \varepsilon}{2} \right) \int u_{xx}^2 dx + \frac{\alpha}{2\varepsilon} \int \left[\left(u \int_V F(u, x, r) \Omega(r) dr \right)_x \right]^2 dx.
\end{aligned}$$

We continue with the second term

$$\begin{aligned}
&\frac{\alpha}{2\varepsilon} \int \left[\left(u \int_V F(u, x, r) \Omega(r) dr \right)_x \right]^2 dx \\
&\leq \frac{\alpha}{2\varepsilon} \int u_x^2 \left(\int_V F \Omega dr \right)^2 dx + \frac{\alpha}{\varepsilon} \int \left(u u_x \int_V F \Omega dr \frac{d}{dx} \int_V F \Omega dr \right) dx \\
&\quad + \frac{\alpha}{2\varepsilon} \int u^2 \left(\frac{d}{dx} \int_V F \Omega dr \right)^2 dx \\
&\leq \left(\frac{\alpha}{2\varepsilon} + \frac{\alpha}{2\varepsilon} \right) \int u_x^2 \left(\int_V F \Omega dr \right)^2 dx + \left(\frac{\alpha}{2\varepsilon} + \frac{\alpha}{2\varepsilon} \right) \int u^2 \left(\frac{d}{dx} \int_V F \Omega dr \right)^2 dx \\
&\leq C(1 + |u|_2^2) \int u_x^2 dx + C(1 + \|u\|^2) \int u^2 dx \\
&\leq C(1 + |u|_2^2) (1 + \|u\|^2) \\
&\leq C(1 + e^{2c_1 t} |u_0|_2^2) (1 + \|u\|^2).
\end{aligned}$$

Now we choose $\varepsilon = \frac{2D}{\alpha}$ such that the first term in (4.3) vanishes and we obtain

$$\frac{d}{dt} \|u\|^2 \leq A(t) + A(t) \|u\|^2,$$

with exponentially growing coefficient function

$$A(t) := C \left(1 + e^{2c_1 t} |u_0|_2^2 \right).$$

Hence, by Grönwall's Lemma, we find that

$$\|u(\cdot, t)\|^2 \leq \Lambda(t) \|u_0\|^2 + \int_0^t \Lambda(t-s) A(s) ds, \quad \Lambda(t) = \exp \left(\int_0^t A(s) ds \right).$$

Integrating $A(s)$ we find constants $c_2, c_3 > 0$ such that

$$\|u(\cdot, t)\| \leq c_2 (\|u_0\| + t) e^{c_3 t}.$$

The H^1/\mathbb{R} -norm, and consequently also the L^∞ -norm, do not grow faster than exponential, hence the solutions are global. \square

5. Numerical solutions. In this section we solve equation (2.2) numerically, for different types of boundary conditions listed in Table 1. We show several examples of adhesive, repulsive and neutral boundary conditions.

5.1. Numerical methods. Equation (2.2) is solved using a method of lines approach, where the spatial derivatives are discretized to yield a large system of time-dependent ODEs (MOL-ODEs). Towards this goal, the domain $[0, L]$ is discretized into a cell-centered grid with uniform length $h = 1/N$, where N is the number of grid cells per unit length. We denote the cell centers as x_i , where $1 \leq i \leq N_1$ (the total number of grid points). The discretization of the advection term utilizes a high-order upwinding scheme augmented with a flux-limiting scheme to ensure positivity of solutions. For full details on the numerical method we refer to [13].

A fast numerical scheme for the non-local term $\mathcal{K}[u]$ is a challenge. In the periodic case the non-local term $\mathcal{K}[u]$ can be efficiently implemented using the Fast Fourier transform (FFT) [14]. For each halfway point between grid points, [14] proposed the approximation

$$a_i := \frac{1}{R} \int_{-R}^R \hat{g}(x_i + h/2 + r) dr = \sum_{l=1}^{N_l} v_{i-l+1} H_l \quad i = 1, \dots, N_1,$$

where H_l are the weights of a piece-wise linear reconstruction of $H(x)$, and where the coefficients v_i are defined by

$$v_i = \frac{1}{R} \int_{-R}^R \Phi \left(i + \frac{r}{h} \right) \Omega(r) dr,$$

where $\Phi(\cdot)$ is a piece-wise linear function. The coefficients v_i can be precomputed at the beginning of a numerical simulation. This means that the computation of a_i can be summarized as a matrix-vector product $\vec{a} = V \vec{H}$ for a matrix $V = (v_{il}) \in \mathbb{R}^{N_1 \times N_1}$. The use of the FFT to accelerate this matrix vector product [14] is well known.

However, in our case the integration limits in $\mathcal{K}[u]$ are spatially dependent near the domain boundary. Thus, near the boundary the FFT can no longer be employed.

We retain the speed advantage the FFT offers, by continuing to use it far away from the boundary (at least one sensing radius). Near the boundary we compute the integration weights v_i for every point and use a matrix-vector product to compute the non-local term in the boundary region. The integration weights near the boundary are given by

$$v_i = \frac{1}{R} \int_{f_1(x_i)}^{f_2(x_i)} \Phi\left(i + \frac{r}{h}\right) \Omega(r) dr.$$

The MOL-ODEs are integrated using the ROWMAP stiff system integration [28] (we use the implementation by the authors¹). This integrator is commonly used to integrate the possibly stiff MOL-ODEs obtained by discretizing PDEs [13, 15, 22, 17].

Model Parameter	Value
Domain Size L	5.0
Domain subdivisions per unit length	128
Diffusion coefficient D	1.0
Adhesion strength coefficient α	varies
Sensing radius R	1.0
Initial conditions (IC)	$1 + \xi$, $\xi \sim \mathcal{N}(0, 1)$
Method error tolerance v_{tol}	10^{-5}
Final simulation time t_f	25

Table 2: Common parameters for the numerical solutions.

5.2. Solutions on a periodic domain. As a control case, we show typical solutions of equation (2.1) on a periodic domain first. In this case we use the sensing domain $E_1(x)$ (see Example 2.1). An extensive bifurcation analysis of the periodic case is given in [7] and we know that the first three bifurcation points from the homogeneous solution are located at

$$\alpha_1 = \frac{16\pi^2}{25(5 - \sqrt{5})}, \quad \alpha_2 = \frac{64\pi^2}{25(5 + \sqrt{5})}, \quad \alpha_3 = \frac{144\pi^2}{25(5 + \sqrt{5})}.$$

This roughly means that $\alpha_1 \sim 2.28$, $\alpha_2 \sim 3.49$, $\alpha_3 \sim 7.85$. For all subsequent numerical simulations we pick a value of α from each of the intervals $(0, \alpha_1)$, (α_1, α_2) , and (α_2, α_3) . The numerical solutions of equation (2.1) with periodic boundary conditions are shown in Figure 4. We identify three important features in these solutions. Firstly, for values of α below the first bifurcation point, the solution is constant. Secondly, as predicted by the bifurcation analysis in [7], a single peak forms between the first and second bifurcation point. Finally, we note that due to the translational symmetry permitted by the periodic boundary conditions, the solution peak may form at any location within the domain. Higher bifurcation points lead to a larger number of

¹http://www.mathematik.uni-halle.de/wissenschaftliches_rechnen/forschung/software/

aggregations in the domain. The local maxima have a uniform distance and they can arise anywhere in the domain due to rotational symmetry [7].

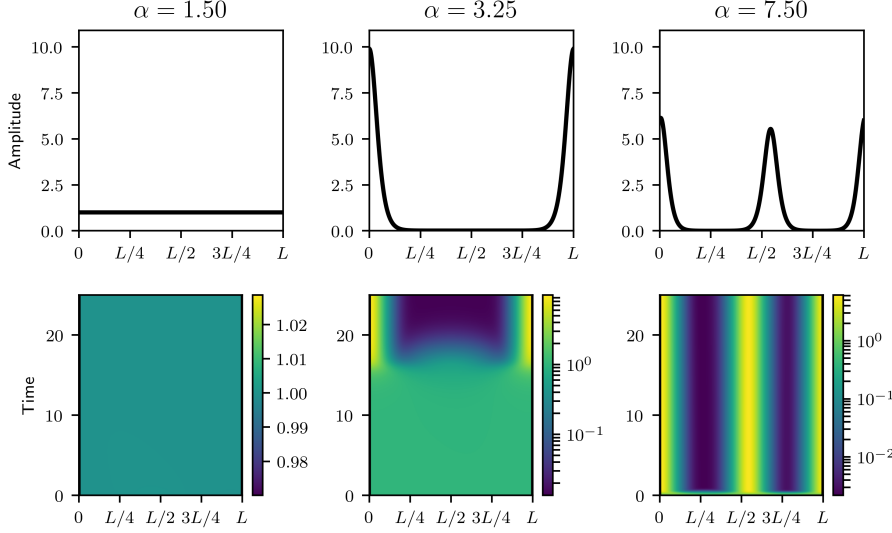


Fig. 4: Numerical solutions of equation (2.1) subject to periodic boundary conditions (see Example 2.1). In the top row we show the final solution profiles, while below are the kymographs. (Left) $\alpha = 1.5$, (Middle) $\alpha = 3.25$, (Right) $\alpha = 7.5$.

5.3. Solutions with No-Flux boundary conditions. We compute numerical solutions for equation (2.1) with the no-flux sensing domain $E_3(x)$ (see Example 2.3). The numerical solutions are shown in Figure 5. Comparing these no-flux solutions to the periodic solution in Figure 4 we identified three differences. First, for $0 < \alpha < \alpha_1$ the solution is no longer constant. In fact the constant solution is now only a solution for $\alpha = 0$. In particular, we note that the solution decreases near the boundary, indicating that the boundary is repulsive. The repulsive nature of the boundaries appears to speed up peak formation in the no-flux case, compared to the periodic case. Second for $\alpha > \alpha_1$ the final no-flux solution profiles correspond to those in the periodic case. Since the no-flux boundary conditions break the translational symmetry observed in the periodic case, the locations of the peaks are fixed in the no-flux case. Finally, we note that while the bifurcation analysis carried out in [7] cannot be straightforwardly extended to the no-flux situation, the numerical results suggest that the bifurcation points are similar.

5.4. Solutions of the adhesive and repulsive boundaries. In this section we demonstrate numerical solutions of with the so called weakly adhesive boundary conditions i.e. sensing domain $E_4(x)$ (see Example 2.5). In particular, we consider the situation in which the constructed $\mathcal{K}[u]$ does not satisfy condition (2.5) i.e. the dependent case. Since in this case the adhesive and diffusive fluxes depend on each other, the existence of solutions in this case are not included in the theoretical results in this paper. However, since we can compute solutions in this case numerically, we explore their possible solutions numerically. As before we distinguish between two

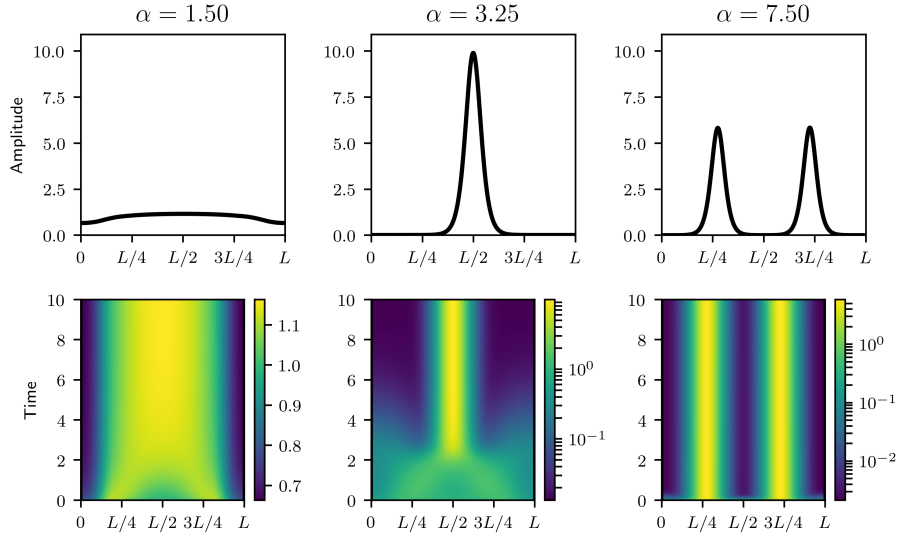


Fig. 5: Numerical solutions of equation (2.1) subject to no-flux boundary conditions with $E_3(x)$ (see Example 2.3). In the top row we show the final solution profiles, while below are the kymographs. (Left) $\alpha = 1.5$, (Middle) $\alpha = 3.25$, (Right) $\alpha = 7.5$.

types of boundaries (1) attractive boundaries $\beta > 0$ and (2) repulsive boundaries $\beta < 0$. The numerical solutions are shown in Figure 6 and Figure 7 respectively.

When the adhesive strength is weak, $\alpha < \alpha_1$, we note that the solution either accumulates (adhesive boundary) or is repelled from the boundary (repulsive boundary), while far away from the boundaries the solutions are constant. These solutions are reminiscent of the menisci which form at a liquid solid interface (e.g. water-glass or mercury-glass). It is well known that the meniscus is concave whenever the liquid-solid adhesion is stronger than liquid-liquid cohesion, while it is convex whenever liquid-liquid cohesion is weaker than liquid-solid adhesion.

For stronger adhesive strength, $\alpha > \alpha_1$, we once again observe the formation of peaks with fixed locations. In the case with adhesive boundary conditions we always find two half peaks on the boundary, while in the repulsive boundary case both peaks form in the domain's interior. Once again the periodic bifurcation analysis appears to be a good predictor of the bifurcation points with different boundary conditions.

6. Conclusions. In the past due to the challenges in construction of boundary conditions, the non-local adhesion model was only considered on unbounded domains or with periodic boundary conditions. However, correct adhesive-boundary interactions are important in biological systems such as during zebrafish development. Here we considered the formulation of no-flux boundary conditions for the non-local adhesion model (1.1), and established the global existence and uniqueness of solutions of (2.1). Thus our work here significantly extends our methods of modelling cell adhesion. We considered two possible methods of extending the non-local adhesion operator (1) by treating the adhesion and diffusion flux as independent, and (2) having the two fluxes depend on each other.

In the independent flux case, we impose standard Neumann boundary conditions

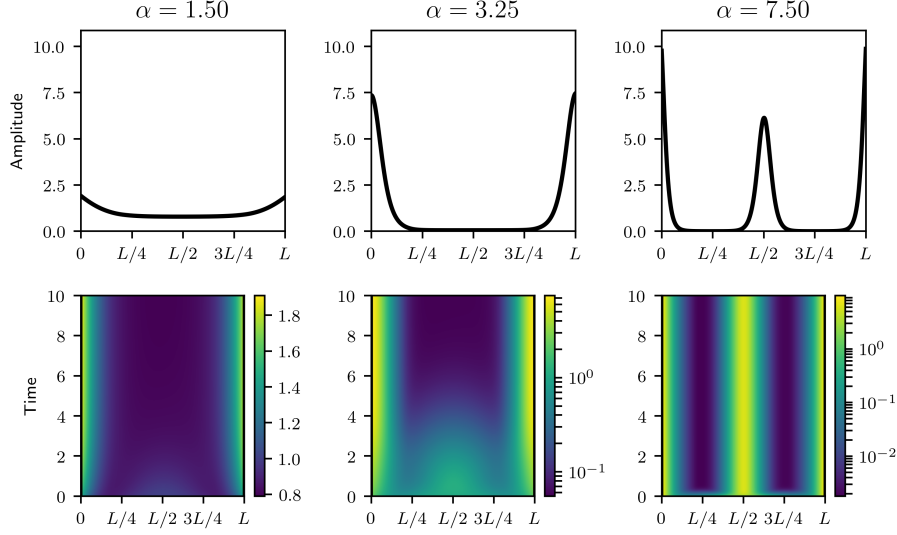


Fig. 6: Numerical solutions of equation (2.1) subject to adhesive boundary conditions (see Example 2.5) with $\beta = 2$. In the top row we show the final solution profiles, while below are the kymographs. (Left) $\alpha = 1.5$, (Middle) $\alpha = 3.25$, (Right) $\alpha = 7.5$.

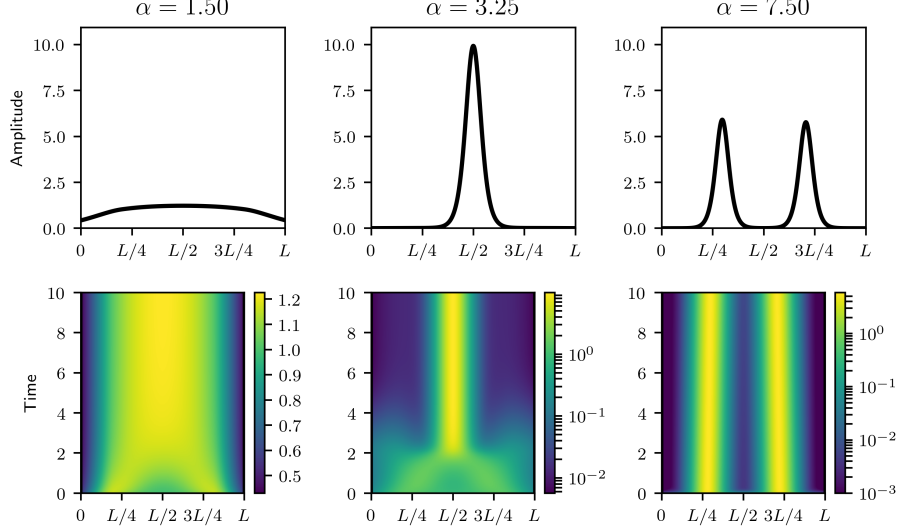


Fig. 7: Numerical solutions of equation (2.1) subject to repulsive boundary conditions (see Example 2.5) with $\beta = -1$. In the top row we show the final solution profiles, while below are the kymographs. (Left) $\alpha = 1.5$, (Middle) $\alpha = 3.25$, (Right) $\alpha = 7.5$.

for the cell population $u(x, t)$, while the behaviour of the non-local operator \mathcal{K} near the

boundary is built into the operator itself. For these no-flux boundary conditions, we establish the global existence of solutions, using standard methods from semi-group theory. While the argument itself is standard, it relies on the novel computation of the weak derivative of the non-local term and its estimates.

The numerical solutions demonstrate that due to the no-flux boundary conditions the translational symmetry observed in the periodic case is broken, and that peaks form at precisely defined locations. This is significant in many biological systems in which combinations of repellent boundaries together with cell-cell adhesion are used to precisely position pre-cursor cells of organs [25]. Repulsive boundaries also accelerated the formation of adhesive cell clusters away from the boundary.

Our existence theory is currently limited to the situation in which the diffusive and adhesive flux are independently zero on the domain's boundary. In particular, the adhesive / repulsive boundary conditions from Example 2.5 are not covered by our theory except for one particular choice for β . It is therefore highly desirable to extend the existence theory to include the cases of Example 2.5. In this case, we must solve a non-local equation (1.1), subject to non-local Robin boundary conditions (2.8). This is a challenging problem. A starting point may be the recent work by [3], who studied the semi-group originating from an elliptic operator on a bounded domain with a linear non-local Robin type boundary condition. As our Robin condition (2.8) is non-linear, the methods of [3] will not directly apply and non-linear methods need to be developed.

Acknowledgments. AB gratefully acknowledges support from a NSERC post-doctoral fellowship. TH gratefully acknowledges support from an NSERC discovery grant.

REFERENCES

- [1] H. AMANN, *Linear and Quasilinear Parabolic Problems: Volume I: Abstract Linear Theory*, vol. 1, Springer Science & Business Media, 1995.
- [2] V. ANDASARI AND M. A. J. CHAPLAIN, *Intracellular modelling of cell-matrix adhesion during cancer cell invasion*, Mathematical Modelling of Natural Phenomena, 7 (2012-01), pp. 29–48, <https://doi.org/10.1051/mmnp/20127103>.
- [3] W. ARENDT, S. KUNKEL, AND M. KUNZE, *Diffusion with nonlocal Robin boundary conditions*, Journal of the Mathematical Society of Japan, 70 (2018), pp. 1523–1556.
- [4] N. J. ARMSTRONG, K. J. PAINTER, AND J. A. SHERRATT, *A continuum approach to modelling cell-cell adhesion.*, Journal of Theoretical Biology, 243 (2006), pp. 98–113, <https://doi.org/10.1016/j.jtbi.2006.05.030>.
- [5] N. J. ARMSTRONG, K. J. PAINTER, AND J. A. SHERRATT, *Adding adhesion to a chemical signaling model for somite formation.*, Bulletin of Mathematical Biology, 71 (2009-01), pp. 1–24, <https://doi.org/10.1007/s11538-008-9350-1>.
- [6] V. BITSOUNI, M. A. J. CHAPLAIN, AND R. EFTIMIE, *Mathematical modelling of cancer invasion: The multiple roles of $\text{tgf-}\beta$ pathway on tumour proliferation and cell adhesion*, Mathematical Models and Methods in Applied Sciences, 27 (2017), pp. 1929–1962, <https://doi.org/10.1142/S021820251750035X>.
- [7] A. BUTTENSCHÖN AND T. HILLEN, *Non-local cell adhesion models: Steady states and bifurcations*, in preparation, (2019).
- [8] A. BUTTENSCHÖN, T. HILLEN, A. GERISCH, AND K. J. PAINTER, *A space-jump derivation for non-local models of cell-cell adhesion and non-local chemotaxis*, Journal of Mathematical Biology, (2017), <https://doi.org/10.1007/s00285-017-1144-3>.
- [9] J. A. CARRILLO, H. MURAKAWA, M. SATO, H. TOGASHI, AND O. TRUSH, *A population dynamics model of cell-cell adhesion incorporating population pressure and density saturation*, arXiv preprint arXiv:1901.02919, (2019).
- [10] M. A. J. CHAPLAIN, M. LACHOWICZ, Z. SZYMANSKA, AND D. WRZOSEK, *Mathematical modelling of cancer invasion: the importance of cell-cell adhesion and cell-matrix adhesion*, Mathematical Models and Methods in Applied Sciences, 21 (2011-04), pp. 719–743,

- <https://doi.org/10.1142/S0218202511005192>.
- [11] P. DOMSCHKE, D. TRUCU, A. GERISCH, AND M. A. J. CHAPLAIN, *Mathematical modelling of cancer invasion: Implications of cell adhesion variability for tumour infiltrative growth patterns.*, Journal of Theoretical Biology, 361C (2014-07), pp. 41–60, <https://doi.org/10.1016/j.jtbi.2014.07.010>.
 - [12] R. C. FETEAU AND M. KOVACIC, *Swarm equilibria in domains with boundaries*, SIAM Journal on Applied Dynamical Systems, 16 (2017), pp. 1260–1308.
 - [13] A. GERISCH, *Numerical Methods for the Simulation of Taxis Diffusion Reaction Systems*, phd, Martin-Luther-Universitat Halle-Wittenberg, 2001.
 - [14] A. GERISCH, *On the approximation and efficient evaluation of integral terms in pde models of cell adhesion*, IMA Journal of Numerical Analysis, 30 (2010), pp. 173–194, <https://doi.org/10.1093/imanum/drp027>.
 - [15] A. GERISCH AND M. A. J. CHAPLAIN, *Mathematical modelling of cancer cell invasion of tissue: local and non-local models and the effect of adhesion.*, Journal of Theoretical Biology, 250 (2008-02), pp. 684–704, <https://doi.org/10.1016/j.jtbi.2007.10.026>.
 - [16] A. GERISCH AND K. J. PAINTER, *Mathematical modeling of cell adhesion and its applications to developmental biology and cancer invasion*, in Cell Mechanics: From Single Scale-Based Models to Multiscale Modelling, A. Chauvière, L. Preziosi, and C. Verdier, eds., CRC Press, 2010, pp. 319–350.
 - [17] T. HILLEN AND K. J. PAINTER, *Transport and anisotropic diffusion models for movement in oriented habitats*, in Dispersal, individual movement and spatial ecology: A mathematical perspective, M. A. Lewis, P. Maini, and S. Petrovskii, eds., vol. 2071, Springer, 2013, pp. 177–222, https://doi.org/10.1007/978-3-642-35497-7_7.
 - [18] T. HILLEN, K. J. PAINTER, AND M. WINKLER, *Global solvability and explicit bounds for a non-local adhesion model*, submitted, (2017).
 - [19] H. MURAKAWA AND H. TOGASHI, *Continuous models for cell-cell adhesion*, Journal of Theoretical Biology, 374 (2015), pp. 1–12, <https://doi.org/10.1016/j.jtbi.2015.03.002>.
 - [20] J. NECAS, *Direct methods in the theory of elliptic equations*, Springer Science & Business Media, 2011.
 - [21] C. OU AND Y. ZHANG, *Traveling wavefronts of nonlocal reaction-diffusion models for adhesion in cell aggregation and cancer invasion*, Canadian Applied Mathematics Quarterly, 21 (2013), pp. 21–62.
 - [22] K. J. PAINTER, *Modelling cell migration strategies in the extracellular matrix*, Journal of Mathematical Biology, 58 (2009), pp. 511–543, <https://doi.org/10.1007/s00285-008-0217-8>.
 - [23] K. J. PAINTER, N. J. ARMSTRONG, AND J. A. SHERRATT, *The impact of adhesion on cellular invasion processes in cancer and development.*, Journal of Theoretical Biology, 264 (2010-06), pp. 1057–67, <https://doi.org/10.1016/j.jtbi.2010.03.033>.
 - [24] K. J. PAINTER, J. M. BLOOMFIELD, J. A. SHERRATT, AND A. GERISCH, *A nonlocal model for contact attraction and repulsion in heterogeneous cell populations*, Bulletin of Mathematical Biology, 77 (2015), pp. 1132–1165, <https://doi.org/10.1007/s11538-015-0080-x>, <https://doi.org/10.1007/s11538-015-0080-x>.
 - [25] A. PAKSA, J. BANDEMER, B. HOECKENDORF, N. RAZIN, K. TARBASHEVICH, S. MININA, D. MEYEN, A. BIUNDO, S. A. LEIDEL, N. PEYRIÉRAS, N. S. GOV, P. J. KELLER, AND E. RAZ, *Repulsive cues combined with physical barriers and cell-cell adhesion determine progenitor cell positioning during organogenesis*, Nature Communications, 7 (2016), pp. 1–14, <https://doi.org/10.1038/ncomms11288>.
 - [26] J. A. SHERRATT, S. A. GOURLEY, N. J. ARMSTRONG, AND K. J. PAINTER, *Boundedness of solutions of a non-local reaction-diffusion model for adhesion in cell aggregation and cancer invasion*, European Journal of Applied Mathematics, 20 (2008-11), p. 123, <https://doi.org/10.1017/S0956792508007742>.
 - [27] M. STEINBERG, *On the mechanism of tissue reconstruction by dissociated cells i. population kinetics, differential adhesiveness, and absence of directed migration*, Proc. Nat. Acad. Sci., 48 (1962), pp. 1577–1582.
 - [28] R. WEINER, B. A. SCHMITT, AND H. PODHAISKY, *Rowmap—a row-code with krylov techniques for large stiff odes*, Applied Numerical Mathematics, 25 (1997), pp. 303–319, [https://doi.org/10.1016/S0168-9274\(97\)00067-6](https://doi.org/10.1016/S0168-9274(97)00067-6).
 - [29] L. WU AND D. SLEPČEV, *Nonlocal interaction equations in environments with heterogeneities and boundaries*, Communications in Partial Differential Equations, 40 (2015), pp. 1241–1281.